PROCEEDINGS OF ECOS 2023 - THE 36TH INTERNATIONAL CONFERENCE ON
EFFICIENCY, COST, OPTIMIZATION, SIMULATION AND ENVIRONMENTAL IMPACT OF ENERGY SYSTEMS
25-30 JUNE 2023, LAS PALMAS DE GRAN CANARIA, SPAIN

Energy-power relations and Ragone plots for packed bed thermal energy storage

Inga Beyers[a], Astrid Bensmann[b] and Richard Hanke-Rauschenbach[d]

[a] Leibniz University Hannover, Institute of Electric Power Systems, Hannover, Germany, beyers@ifes.uni-hannover.de
[b] Leibniz University Hannover, Institute of Electric Power Systems, Hannover, Germany, astrid.bensmann@ifes.uni-hannover.de, CA
[c] Leibniz University Hannover, Institute of Electric Power Systems, Hannover, Germany, hanke-rauschenbach@ifes.uni-hannover.de

Abstract:

Packed beds are essential components for future utility-scale long duration energy storage, such as A-CAES and Carnot batteries, and are expected to operate under a large variety of operating conditions. The operating behaviour can be visualised compactly within Ragone plots, which show the extractable energy over a range of discharge powers. They can additionally demonstrate the effect of different operational limits. Ragone plots are a well-known framework within electrochemical energy storage, but have not been applied to packed bed thermal energy storage. In this work, Ragone plots of packed beds are developed, to quantify off-design behaviour and the energy-power trade-off. For this purpose, a one-dimensional, two-phase, transient, Schumann-style model for a non-pressurized packed bed is implemented in the modelling language Modelica. It is charged up to a nominal thermal energy of 100 MWh and subsequently discharged with two different discharge regimes, namely a constant mass flow discharge or a constant heat tranfer rate discharge. The shape of the obtained Ragone plots is characterised by limited self-discharge and little decline in available energy at high constant mass flow discharges. The enforcement of the mass flow limit and imperfect heat transfer dynamics lead to a residual thermal energy within the storage, which can be extracted at lower heat transfer rates. Analogies to electrochemical energy storage are drawn, where polarisation causes a conceptually similar residual energy.

Keywords:

Energy Storage, Packed Bed, Thermal Energy Storage, Ragone plots, Energy-Power relations

1. Introduction

In this paper, a packed bed thermal energy storage (TES) is studied and characterised within the Ragone plot framework and analogies between electrochemical energy storage are demonstrated. This is important since packed beds are considered strong contenders for TES components in future long-duration energy storage, such as Carnot batteries [1], compressed air energy storage (CAES) [2] and in the decarbonisation of industrial heat [3], due to their favourable characteristics. These characteristics include excellent heat transfer, low material costs, a low environmental impact, a high operational temperature range and high output temperature levels, due to thermal stratification. The study of packed beds has attracted considerable research attention, especially their modelling [4, 5], parametric optimisation [6] and performance aspects [7].

The Ragone plot shows the available energy as a function of discharge power and thus characterises the inherent energy-power trade-off of energy storage [8]. It is a very fundamental relation and can be construed as a “common language” of energy storage [9]. The characterisation of packed beds within this framework therefore enables the direct comparison with different energy storage technologies, across their respective fields.

The Ragone plot was first introduced by David Ragone in 1968 [10], and over the following years established itself a concept in the field of electrochemical energy storage, e.g. batteries and supercapacitors. They have recently also been applied in the field of TES (and associated technologies). Latent heat TES has been characterised with Ragone plots by [11–13]. Of these, Woods et. al. [12] presents a comprehensive Ragone plot analysis of different phase change materials. Here, the energy-power trade-off in a finite volume is shown, whereby heat transfer is improved at the cost of energy capacity. The publication lays the foundation for Ragone plot characterisation of TES as standalone components. The thermal energy is extracted at different constant heat transfer rates $\dot{q}$, as the thermal equivalent to electric power.

Christen [9] characterised pumped thermal energy storage (PTES) with both latent and sensible TES via Ragone plots. Here the TES is not characterised directly, but as a component within electric energy storage.

https://doi.org/10.52202/069564-0193

The analysis employs endoreversible thermodynamics [14] (perfect heat engine with irreversible heat transfer) to estimate the electric power delivered. Further, a lumped-model approach is used, which means there is no spatial temperature variation. This implies perfect mixing within the sensible TES, where the output temperature decays during the entire discharge process. In contrast, in a thermally stratified packed bed, a high, nearly constant output temperature can be held over the first part of a discharge until thermal front has migrated towards the outlet. A packed bed therefore lies somewhere between mixed sensible and latent TES in terms of maintaining high output temperatures, which is beneficial in a thermodynamic power cycle.

The contribution of this paper is to conduct the first analysis of packed beds within the Ragone plot framework, as this has not been attempted before. For this, a state-of-the-art packed bed model is used. Analogies between packed bed TES and electrochemical energy storage discharge modes are developed, to effectively translate the Ragone plot framework. An assessment of off-design performance of packed beds follows, both in the context of pure thermal energy storage and as a thermal reservoir for a power cycle. The remainder of the paper is structured as follows: Section 2 describes the methodology of the Ragone plot and the employed packed bed model. Section 3 shows the obtained results and highlights key findings. Section 4 summarises the results and derives the conclusion from the presented analysis.

2. Methodology

2.1. The Ragone plot framework and discharge regimes

A Ragone plot essentially is a collection of energy-power value pairs from full discharges of any kind of energy storage. These value pairs form a Ragone curve or energy-power (E-P) curve. Ragone curves are often presented as specific values, based on storage mass (gravimetric energy and power density) or on storage volume (volumetric energy and power density) However, absolute values are also used, depending on what makes most sense in the given context.

Christen and Carlen [8] have expressed the Ragone curve as stemming from constant-power (CP) discharges, where a constant power P can be applied to an fully charged energy storage for a finite time t_{end} until an internal operating limit terminates the discharge. This results in the following E-P relation:

$$E(P) = P \cdot t_{\text{end}}(P) \tag{1}$$

However, the electrochemical ES community routinely characterises batteries with constant-current (CC) discharges. This does not result in an unambiguous energy-power point, because the power varies in the course of this type of discharge. In these cases, the E-P value pair for a constant current I is obtained by averaging the power over the discharge time, resulting in

$$E(I) = P_{\text{ave}}(I) \cdot t_{\text{end}}(I) \tag{2}$$

These two fundamental discharge regimes found in batteries (CC/CP) have direct equivalents in packed bed TES, which are all shown together for illustration purposes in Fig. 1. All subfigures show the potential variable of the energy storage (voltage U for the lithium-ion battery and the specific enthalpy difference Δh of the fluid at inlet and outlet for the packed bed) and the flow variable (current I for the lithium-ion battery and mass flow rate $\dot{m}$ for the packed bed) over the course of the discharge time.

Fig. 1 a) and b) are the respective constant flow discharge regimes. In a CC-discharge of a lithium-ion-battery in a), the output voltage decays until the discharge is terminated by reaching the predefined operating limit U_{min}. The output power $P(t) = U(t) \cdot I$ also decays. Analogously, in Fig. 1 b) Δh decays during the constant mass flow discharge (referred to as "CF"-discharge hereafter), until termination at T_{min}. Here the potential variable and flow variable multiplied result in a decaying heat transfer rate $\dot{q}(t) = \Delta h(t) \cdot \dot{m}$ delivered to the application. The Ragone plot from a CF-discharge of a packed bed can thus be expressed as:

$$E(\dot{m}) = \dot{q}_{\text{ave}}(\dot{m}) \cdot t_{\text{end}}(\dot{m}) \tag{3}$$

To compensate the decaying voltage in lithium-ion batteries, the current can be increased during the discharge to deliver a constant power, see Fig. 1 c). The packed bed equivalent is increasing the mass flow to compensate the decaying Δh and deliver a constant heat transfer rate $\dot{q}$, referred to as a "CQ"-discharge hereafter. The CP and CQ discharge regimes have a higher control effort, but are necessary if load-following must be achieved [9]. Here, the discharge can be terminated by reaching a potential variable limit (i.e. U_{min} or T_{min}) or by reaching a flow variable limit, here I_{max} or $\dot{m}_{\text{max}}$. The Ragone plot derived from multiple CQ-discharges become simply:

$$E(\dot{q}) = \dot{q} \cdot t_{\text{end}}(\dot{q}) \tag{4}$$

It must be noted, that in [12], the constant heat transfer rate for the latent heat TES Ragone plots is realised by adjusting the inlet temperature instead of the mass flow. We consider an increase in mass flow better suited for

https://doi.org/10.52202/069564-0193

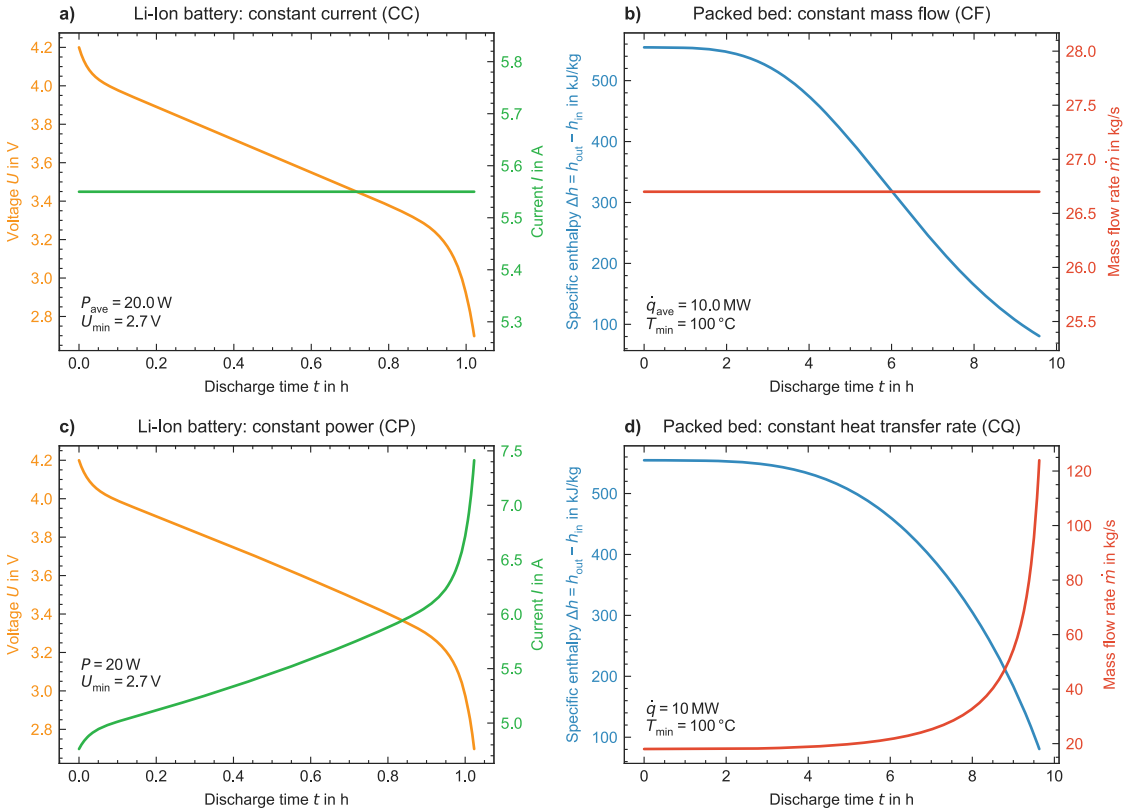

Figure 1: Equivalent discharge regimes for electrochemical ES, represented here by a lithium-ion battery, in a) and c) and packed bed TES in b) and d).

this analysis. The adjustment of the inlet temperature premises another heat source/sink apart from the TES itself, which is deemed impractical. In the course of this analysis, a representative packed bed will be studied under both CF and CQ discharge regimes.

2.2. Packed bed sizing

The packed bed is sized for a nominal energy capacity E_{nom} = 100 MWh in a top-down design approach, with inlet temperatures assumed at T_{in} = T_{max} of 550 °C during charge and 20 °C = T_{amb} = T_{min} for discharge. The packed bed is considered a non-pressurised rock-air system. The amount of rock mass m_s needed is calculated from [6] as follows:

$$E_{nom} = \frac{m_s}{\beta} \cdot c_{p,s} \cdot (T_{max} - T_{min}) \tag{5}$$

The packed bed is oversized by a factor β = 1.5 to prevent energy and exergy lost by exiting hot air, in accordance to results from Cardenas et. al. [6]. The basic geometry, namely radius r and height H is calculated via (6) and (7), for an aspect ratio of α = 0.7 [6].

$$r = \left(\frac{m_s}{2\pi \cdot \alpha \cdot \rho_s \cdot (1 - \epsilon)} \right)^{1/3} \tag{6}$$

$$H = 2 \cdot r \cdot \alpha \tag{7}$$

The nominal discharge time is set at t_{nom} = 10 hours. From this, the nominal mass flow $\dot{m}_{nom}$ can be calculated via the following simplified relation:

$$\dot{m}_{nom} = \frac{E_{nom}}{t_{nom} \cdot \overline{c_{p,f}} \cdot \overline{\Delta T}} = \frac{E_{nom}}{t_{nom} \cdot \frac{c_{p,f}(T_{max}) + c_{p,f}(T_{min})}{2} \cdot \frac{(T_{max} - T_{min})}{2}} \tag{8}$$

The according specific mass flow G_{nom} is:

$$G_{nom} = \frac{\dot{m}_{nom}}{2\pi \cdot r^2} \tag{9}$$

The key design parameters of the packed bed are summarised in Table 1, where the values are colour-coded according to their degree of freedom in the design process. The design process chronology is from the top to bottom of the table.

Table 1: Overview over packed bed design parameters, colour-coded according to their degree of freedom in the design process. With = high degree of freedom, = limited degree of freedom and = resulting value.

Design parameter	Unit	Value	Source
E_{nom}	MWh	100	
T_{min}	°C	20	
T_{max}	°C	550	[4]
solid specific heat capacity $c_{p,s}$	J/kgK	960	[15]
solid density ρ_s	kg/m^3	2560	[15]
rock mass m_s	t	1061.3	
aspect ratio α	-	0.7	[6]
oversize factor β	-	1.5	[6]
porosity ϵ	-	0.40	[4]
rock diameter d	m	0.02	[4]
radius r	m	5.40	
height r	m	10.80	
cross section A	m^2	91.47	
t_{nom}	h	10	
nominal mass flow $\dot{m}_{nom}$	kg/s	36.33	
nominal specific mass flow G_{nom}	kg/sm^2	0.3972	

The wall is composed of three layers, adopted from [16]: an internal tube, an insulation layer and an outer steel vessel. Their respective parameters are listed in Table 2.

Table 2: Wall composition of packed bed

Design parameter	Unit	Tube	Insulation	Steel vessel
thickness r	m	$0.001 \cdot 2r$	$0.05 \cdot 2r$	$0.001 \cdot 2r$
thermal conductivity k	W/mK	0.12	0.15	20

2.3. Packed bed model description and validation

The Ragone plot analysis is conducted on the basis of a dynamic physical model of the packed bed, according to current standard modelling practise. The model is a transient, two-phase, Schumann-style model, widely used in the study of packed beds. The model is governed by mass conservation and by an separate energy balance for solid and fluid respectively, linked through the convective heat transfer between fluid and solid. The model further considers axial conduction through the solid and losses from fluid to ambient. The equations are taken from [4]. For the fluid phase this is:

$$\epsilon\, \rho_f\, c_{p,f}(T_f)\, A\, \frac{\partial T_f}{\partial t} = h_V\, A\, (T_s - T_f) + c_{p,f}(T_f)\, G\, A\, \frac{\partial T_f}{\partial x} + U_{wall}\, 2\, \pi\, r\, (T_{amb} - T_f) \tag{10}$$

with the volumetric heat transfer coefficient h_V from the correlation of Coutier and Faber [15] and the overall loss coefficient through the wall U_{wall}. U_{wall} is calculated as conduction through a multi-layered cylinder wall [19] with no thermal capacitance of the wall. The convection at the inner wall is from [20], while the convection at the outer wall is considered as free convection near a vertical surface [18]. For the solid phase the energy conservation equation is:

$$(1 - \epsilon)\, \rho_s\, c_{p,s}\, \frac{\partial T_s}{\partial t} = h_V\, (T_s - T_f) + k_{bed}\, \frac{\partial^2 T_s}{\partial x^2} \tag{11}$$

with the axial thermal conductivity of packed bed k_{bed}. This is evaluated according to the model of Zehner, Bauer and Schlünder [18]. The two-phase formulation is important to capture transient effects, i.e. when fluid

https://doi.org/10.52202/069564-0193

and solid are not in thermal equilibrium [17]. The energy E contained in the packed bed is determined via the temperature of the solid [4] and is given in (12). The pressure loss in the packed bed is calculated via the Ergun equation [18].

$$E = \int_0^H \rho_s \, c_{p,s} \, A \, (T_s(x) - T_{amb}) \, dx \tag{12}$$

2.3.1. Implementation

The numerical model is implemented in the acausal, multi-physics modelling language Modelica and solved within the open source modelling environment OpenModelica. As OpenModelica cannot solve partial differential equations (PDE), a finite volume discretisation is applied to (10) and (11) to form a set of coupled ordinary differential equations (ODE), where each control volume is governed by an ODE. The discretisation scheme and structure of the layer-based equations are adopted from [17]. The temperature-dependent thermodynamic properties of air are calculated at every point in time with the integrated "ReferenceAir" medium model contained in the Media library. This is a real gas model for dry air in the range of 130 K to 2000 K, based on Helmholtz equations of state.

2.3.2. Validation

The packed bed model is validated with the experimental data of Meier et. al. [21], further described by Hänchen et. al. [4], by scaling the model to the geometric dimensions specified. The result is shown in Fig. 2. The model shows good thermal agreement, but overestimates pressure losses by approx. 10 %, which is a known effect of the Ergun equation for randomly packed, spherical rock beds [22]. However, the equation is standard practise [18] and agreement is deemed satisfactory for the scope of this work.

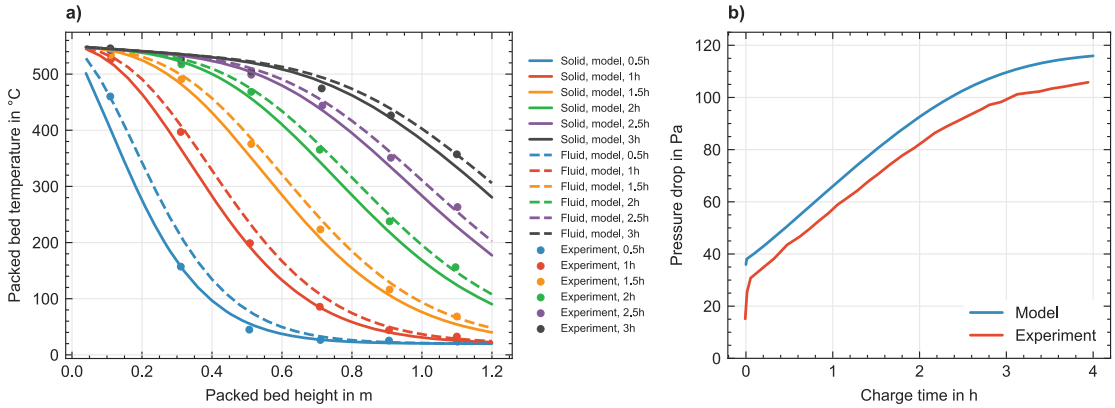

Figure 2: Validation of a) thermocline behaviour and b) pressure drop of the packed bed model with U_{wall} = 0.678 W/m^{2}K at 523 K and a bypass flow of 15 % reported in [4]. Comparison with experimental data from [21]. The model is discretised into 30 layers.

2.4. Consideration of auxiliary components

In a non-pressurised packed bed, airflow is driven by an auxiliary fan/blower and the pressure drop Δp incurred through the bed must be compensated [6]. This must be considered in the Ragone plot analysis, because high mass flows result in higher pressure drops. Additionally, because the mass flow will be varied between discharges in the CF regime and during the course of a discharge in the CQ regime, a reasonable $\dot{m}_{max}$ must be determined. Whether the auxiliary is considered a fan or a blower depends on the pressure ratio, but the distinction is not clear-cut in literature [23]. For simplification purposes, we only refer to "fan" from this point onward.

The required auxiliary fan power is expressed as [24]:

$$P_{aux} = \frac{\dot{V} \cdot \Delta p}{\eta_{fan}} \tag{13}$$

with η_{fan} assumed at 80 % [24] for all operating points. This is a simplification, as the fan will operate in unsteady, off-design conditions. Even in a constant mass flow CF charge/discharge, the pressure loss to be compensated varies in the course of the charge/discharge, as the thermodynamic properties of the fluid inside

the packed bed change. This is also confirmed experimentally in Fig 2 b). The off-design behaviour of fans can be characterised with performance maps, which are usually determined experimentally and are specific to a fan type and geometry. However, with variable speed drives, satisfactory efficiencies can be achieved over a large range of mass flows, respective volume flows [24]. Therefore the consideration with a single efficiency is considerd sufficient and analysis with detailed performance maps is not deemed expedient.

Up to a pressure ratio of 1.3, air can be assumed as a incompressible medium [25], and therefore P_{aux} is calculated with the volume flow at inlet in 13. This is often viewed as the limit between fans and compressors [25]. This limit adopted here as the maximum allowable fan pressure ratio and higher pressure losses are a priori deemed impractical. From this condition, a maximum mass flow $\dot{m}_{max}$ can be iteratively determined from simulation runs, resulting in $\dot{m}_{max} = 158\,\mathrm{kg/s}$ or $4.3 \cdot \dot{m}_{nom}$. The maximum specific mass flow is thus $G_{max} = 1.727\,\mathrm{kg/sm^2}$.

3. Results and Discussion

3.1. Ragone plots from CF-discharge

In a first step, Ragone plots are developed from multiple constant mass flow (CF) discharges, as specified in Section 2.1. The packed bed is fully charged to nominal energy, then subsequently immediately discharged until the cut-off temperature is reached. This is repeated multiple times, starting from a mass flow of $0.1 \cdot \dot{m}_{nom}$ up to $\dot{m}_{max} = 4.3 \cdot \dot{m}_{nom}$. The result is shown in Fig. 3 a) for a cut-off temperature of $T_{min} = 20\,^{\circ}\mathrm{C}$ and in b) for $T_{min} = 100\,^{\circ}\mathrm{C}$.

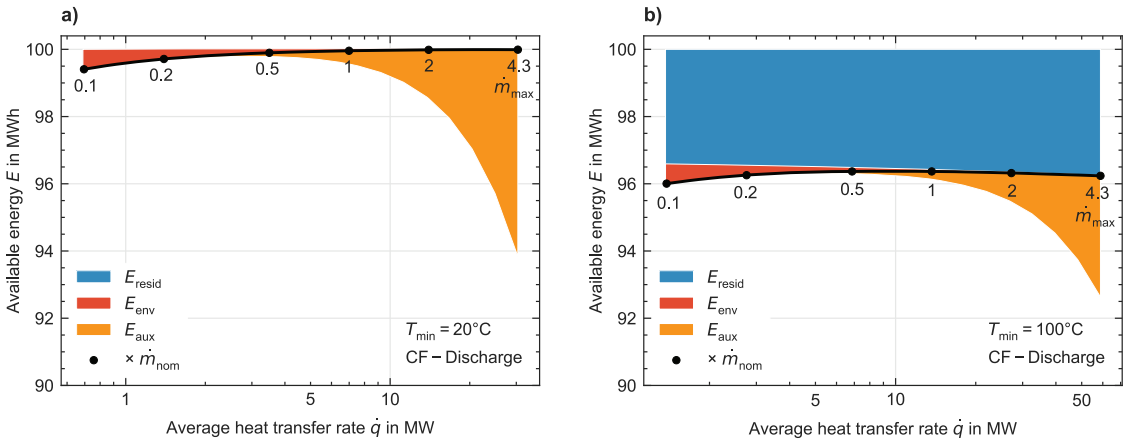

Figure 3: Ragone plots from multiple CF-discharges.

The Ragone curves (in black) show the available thermal energy over the average heat transfer rate. Certain mass flows are demarcated by dots; these are multiples of the nominal mass flow (conceptually similar to the C-rate in lithium-ion batteries). Classically, the Ragone curve is shown without any other descriptive elements. In this case, a novel visualisation is implemented to demonstrate how the Ragone curves are composed. The area above the curve (thermal energy that cannot be extracted) is color-coded, where red equals energy lost to environment and blue is residual energy in the storage. Further included is the electric energy required by the auxiliary fan to achieve the respective mass flows (yellow). This is not subtracted from the Ragone curve, because it does not lessen the available thermal energy, but is included for reference. It rises sharply for higher mass flows.

The Ragone curves confirm known packed-bed qualities. Thermal energy can be contained well, even for long discharge durations at low mass flows, signalled by low losses to the environment. Additionally, higher mass flows don't negatively impact available thermal energy to the extent that, e.g. high currents limit available energy in Li-Ion batteries. The forced convective heat transfer is still very good at high mass flows. Because of these characteristics, the shape of the Ragone curve in the CF-discharge regime is relatively flat. It is important to note that thermal front degradation does not show itself in Fig. 3, because the energy content remains the same and the bed is oversized to the extent that the thermal front degradation does not reach the outlet in the discharge durations considered.

The location of the Ragone curve on the E-Q plane is largely determined by the cut-off temperature. In Fig. 3 a), no thermal energy remains in the packed bed, whereas in Fig. 3 b) the higher cut-off temperature moves the entire Ragone curve downward, resulting in residual thermal energy. This is shown in Fig. 4, for multiple

https://doi.org/10.52202/069564-0193

different T_{min}. The residual energy and energy lost to the environment are not included here for visual clarity, only the auxiliary energy.

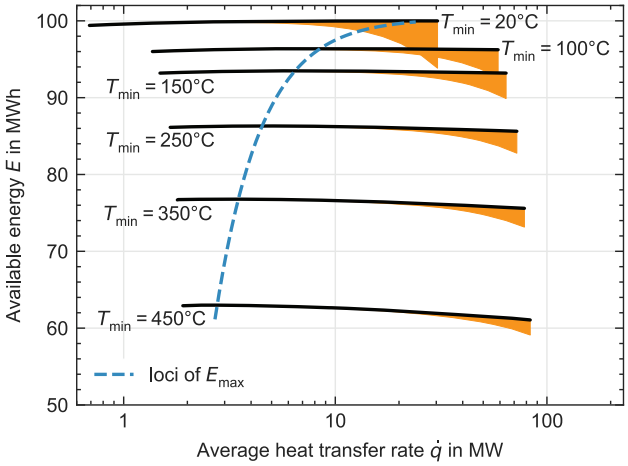

Figure 4: Ragone plots with varying cut-off temperature limits T_{min}.

One thing that becomes clear in Fig. 4, is that there is no single unique assignment between $\dot{q}_{ave}$ and $\dot{m}$. Depending on T_{min} and the resulting discharge end time, a specific $\dot{m}$ might result in different $\dot{q}_{ave}$. Secondly, one can observe a slight decrease in available energy at higher $\dot{q}_{ave}$. This can be attributed to an effect that is equivalent to polarisation in lithium-ion batteries. Polarisation is when charge transfer from and into the electrode cannot keep up with high current demands, resulting in overpotentials [26]. These lead to a premature termination of discharge and cause a residual energy that can only be extracted at lower currents. In the packed bed, imperfect heat transfer dynamics at high mass flow rates results in a temperature difference between fluid and solid. At the end of the discharge, the solid still has a higher temperature, but the fluid outlet temperature is lower and triggers the discharge cut-off. This effect is shown in Fig.5. It shows the temperature difference ΔT between solid and fluid, plotted over the specific mass flow G for several different lower cut-off temperatures.

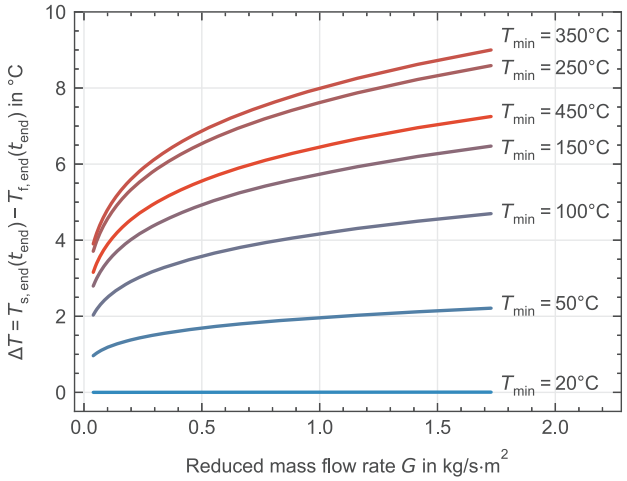

Figure 5: Temperature difference $\Delta T(t_{end})$ between solid and fluid at the end of discharge for different T_{min}.

From Fig.5 it can be seen that higher mass flows generally result in higher ΔT and thus higher "polarisation". But ΔT is also dependent on T_{min}. The temperature difference is highest within the thermocline, and stopping the discharge as the steepest point of the thermocline exits, results in highest ΔT (here at $T_{min} = 350\,°C$). This in turn leads to the highest amount of residual energy due to heat transfer limitations.

https://doi.org/10.52202/069564-0193

3.2. Ragone plots from CQ-discharge

In the second part of the analysis, Ragone plots constant heat transfer rate (CQ) discharges are developed, presented here in Fig. 6. As in Section 3.1., the packed bed is fully charged and immediately discharge until termination by either reaching the predefined maximum mass flow $\dot{m}_{\mathrm{max}}$ or the cut-off temperature T_{min}. This is repeated for multiple heat transfer rates, with the E-Q value pairs forming the Ragone curve. In 6 a), the

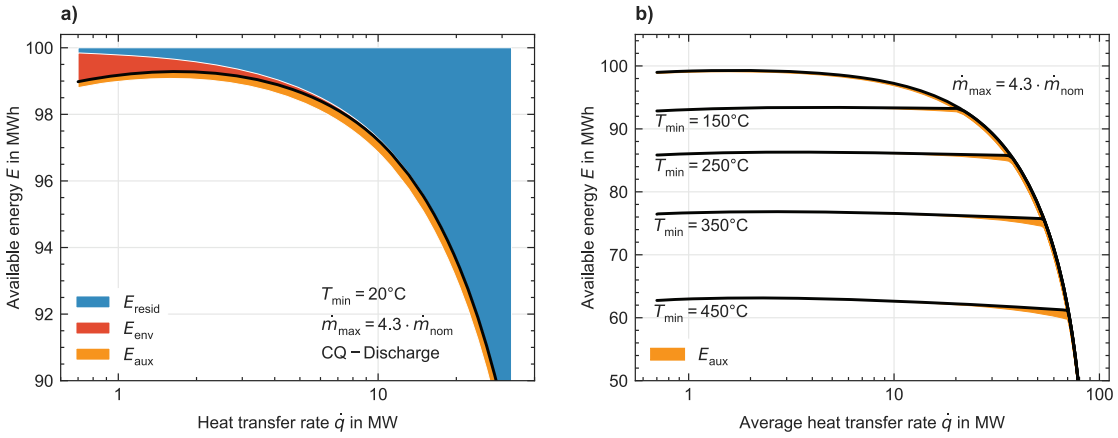

Figure 6: CQ-Ragone plots, curve composition in a) and variation of T_{min}.

Ragone plot for $T_{\mathrm{min}} = 20\,^{\circ}\mathrm{C}$ shows a very different curve, than its CF-counterpart in Fig. 3 a). Here, the minimum temperature cut-off does not come into play, because the Ragone curve (in black) is limited by the maximum mass flow $\dot{m}_{\mathrm{max}}$ in every discharge. As shown in Section 2.1., the mass flow is increases towards the end of the discharge, to compensate the decaying output. In this case, $\dot{m}_{\mathrm{max}}$ is always reached before $T_{\mathrm{min}} = 20\,^{\circ}\mathrm{C}$. This cut-off leaves a residual energy (blue) within the storage that can only be extracted at lower heat transfer rates, even in the case of $T_{\mathrm{min}} = 20\,^{\circ}\mathrm{C}$. The auxiliary energy needed is more evenly distributed, because the fan only operates at high mass flow rates at the end of the discharge.

Figure 6 b) shows the Ragone curves for different lower temperature limits T_{min}. Here, for higher T_{min} limits, the Ragone curves are each composed of two distinct sections, a relatively flat temperature-limited section and a mass-flow-limited section, where the available energy drops quickly. The mass flow limit forms an outer enveloping curve for all the Ragone curves.

It must be noted, that the available energy reaches a limit of 0 at $\dot{q}_{max}$. This is not shown in Fig. 6 b) as it is not considered an actual practical operating point and the axes are identical to the CF-discharge in Fig. 3 b) for comparison purposes. At this point $E \to 0$, $\dot{q}$ is only applied for infinitesimally short discharge duration, and the maximum mass flow limit $\dot{m}_{max}$ is immediately enforced.

3.3. Packed bed as a thermal reservoir for a power cycle

The Ragone plots presented in Section 3.2. and 3.1. show only available energy and do not differentiate between exergy and anergy. This energy-based analysis is valid, as packed beds can be utilised purely in a thermal energy storage context, e.g. in the recuperation of waste heat, that is used to preheat fluid streams at a later point. If desired, energy quality (i.e. exergy) demands can be encoded in these Ragone plots, by setting a certain T_{min}, but this is a quite roundabout way.

Alternatively, a simple way to evaluate the packed bed as a thermal reservoir for a power cycle is to apply a Carnot efficiency $\eta_{\mathrm{carnot}} = 1 - T_{\mathrm{out}}/T_{\mathrm{amb}}$ to the output, which has been employed by [9]. This is a theoretical analysis, as there is no consideration of control regimes or any other irreversibilities apart from those included in the packed bed model, but it is a quick and convenient manner in which to produce electric energy over power Ragone plots, based on a specific TES. Fig. 7 a) shows the result of such an analysis, where the output power P is kept constant, until the storage is unable to deliver it and the discharge is terminated. Unlike the analysis in Section 3.1. and 3.2., the maximum mass flow is set as $\dot{m}_{max} = 1.5\dot{m}_{nom}$ because the achievable mass flow variations are more limited in a power cycle.

Here, also $E(P_{\mathrm{max}}) \to 0$, which Christen [9] generally asserted for sensible heat storage. However, the shape of the Ragone curve is bulged outwards towards higher E and P values, instead of inwards like the mixed sensible TES [9]. The thermal stratification and good heat transfer of the packed bed enable a higher Carnot efficiency over a longer part of discharge. This Ragone plot can easily be compared to the E-P relation of other electric storage technologies, regardless of their functional principle. This is demonstrated in Fig. 7 b), where

https://doi.org/10.52202/069564-0193

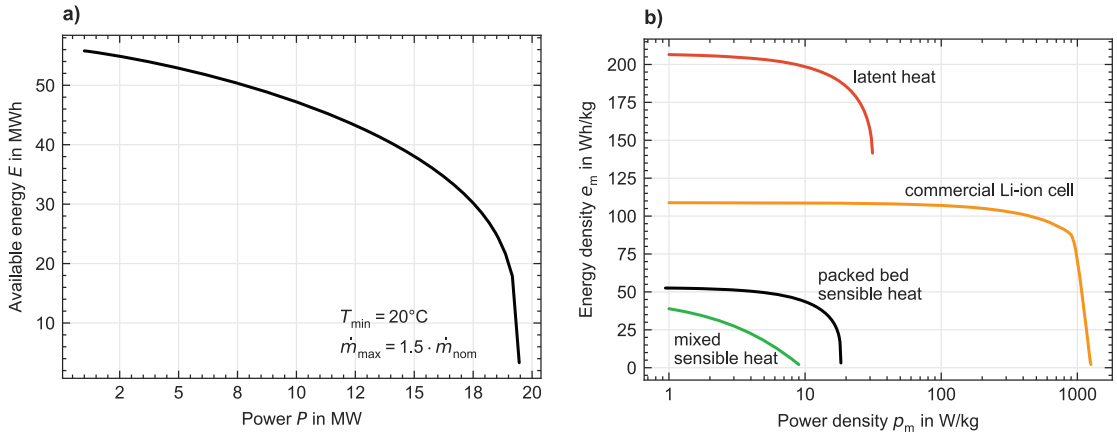

Figure 7: a) Ragone plot from CP-discharge of the 100 MWh packed bed via a Carnot engine. b) Gravimetric Ragone plot of the packed bed-based PTES and comparison to mixed sensible and latent heat PTES from [9], in addition to a commercial Li-ion battery cell.

the specific-value Ragone curves of perfectly mixed sensible and latent heat PTES from [9] are included for comparison purposes, in addition to a commercial Li-ion battery cell. It should be noted that the specific-value Ragone curve of a full Li-ion system with periphery would have lower specific values. The Ragone curve shape of the packed bed PTES underlines its characteristics, as it shares both the property of mixed sensible heat, where $E(P_{max}) \rightarrow 0$, but also the convex Ragone curve shape of latent heat. As a storage technology, packed bed-based PTES have relatively low gravimetric energy and power densities.

3.4. Comments on cyclic stability

Packed bed behaviour is known to reach quasi-stationary cyclic temperature profiles in charge-discharge cycles of constant duration [7]. This is achieved after a certain number of cycles (5-20 cycles is the range typically found in literature). In the packed bed analysed here, the cyclic stability is reached after ten cycles, as shown in Fig. 8. Packed bed analyses are often conducted on the basis of these quasi-stationary temperature pro-

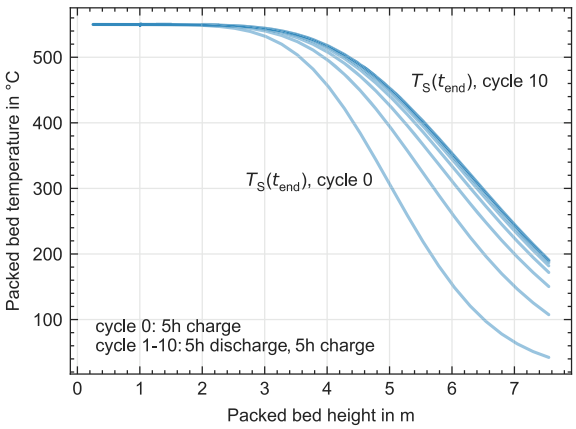

Figure 8: Cyclic stability in the packed bed temperature profile: Final temperature $T_s(t_{end})$ after charge.

files [4, 5, 7], however in case of Ragone plots, we have not integrated this into the analysis. Several issues arise when applying the cycle stability logic into the Ragone framework. Firstly, the stable temperature profile is different for every cycle length [7], introducing an additional level of variability. Secondly, the energy in the packed bed after reaching cyclic thermal stability will differ from the nominal energy. In Fig. 8 it is approx. 25 % higher than E_{nom}. Additionally, the losses incurred along the way by the multiple cycles cannot be cleanly integrated into a subsequent Ragone plot analysis. Cyclic analysis makes sense in a cyclical load regime, e.g. storage for concentrated solar power. However in a thermal load-following paradigm or variable discharge

waste heat output, cyclic operation will not be given in any case. And while the Ragone plot also does not cover all possible load scenarios, its benefit lies in the formulation of a consistent scenario [9] and the comparability to other storage technologies.

4. Conclusions

The presented analysis aimed to evaluate packed bed TES within the Ragone plot framework and draw analogies to the field of electrochemical energy storage. An exemplary 100 MW packed bed model was sized and simulated under different discharge regimes. The main conclusions are derived as follows:

- Two discharge regimes are identified for packed beds, namely CF (constant mass flow) and CQ (constant heat transfer rate), which have direct counterparts (CC and CP) in the field of electrochemical energy storage.
- The energy-power trade-off of packed beds, quantified here with Ragone plots, is low and the analysed packed bed shows good performance over a large range of discharge demands.
- Imperfect heat transfer dynamics cause a residual energy in packed beds, that is conceptually equivalent to polarisation in electrochemical energy storage.
- The Ragone plot framework is well-defined, simple-to-use scenario, that is well-suited for off-design characterisation of TES. This can be done both within the function as pure thermal energy storage and as a thermal reservoir for a power cycle. The obtained results can be compared directly and quantitatively with any other energy storage technology.

Acknowledgments

We thank Alexander Wernke and Fabian Geerling for helpful discussions.

References

[1] Liang T, Vecchi A, Knobloch K, Sciacovelli A, Engelbrecht K, Li Y, et al. *Key components for Carnot Battery: Technology review, technical barriers and selection criteria.* Renewable and Sustainable Energy Reviews. 2022 Jul;163:112478.

[2] Barbour E, Mignard D, Ding Y, Li Y. *Adiabatic Compressed Air Energy Storage with packed bed thermal energy storage.* Applied Energy. 2015 Oct 1;155:804–15.

[3] Manente G, Ding Y, Sciacovelli A. *structured procedure for the selection of thermal energy storage options for utilization and conversion of industrial waste heat.* Journal of Energy Storage. 2022 Jul 1;51:104411.

[4] Hänchen M, Brückner S, Steinfeld A. *High-temperature thermal storage using a packed bed of rocks – Heat transfer analysis and experimental validation.* Applied Thermal Engineering. 2011 Jul;31(10):1798–806.

[5] Mertens N, Alobaid F, Frigge L, Epple B. *Dynamic simulation of integrated rock-bed thermocline storage for concentrated solar power.* Solar Energy. 2014 Dec;110:830–42.

[6] Cárdenas B, Davenne TR, Rouse JP, Garvey SD. *Effect of design parameters on the exergy efficiency of a utility-scale packed bed.* Journal of Energy Storage. 2018 Aug;18:267–84.

[7] McTigue JD, Markides CN, White AJ. *Performance response of packed-bed thermal storage to cycle duration perturbations. Journal of Energy Storage.* 2018 Oct;19:379–92.

[8] Christen T, Carlen MW. *Theory of Ragone plots.* Journal of Power Sources. 2000 Dec;91(2):210–6.

[9] Christen T. *Ragone plots and discharge efficiency-power relations of electric and thermal energy storage devices.* Journal of Energy Storage. 2020 Feb;27:101084.

[10] Ragone DV. *Review of Battery Systems for Electrically Powered Vehicles.* Presented at the Mid-Year Meeting of the Society of Automotive Engineers 1968, p. 680453.

[11] Yazawa K, Shamberger PJ, Fisher TS. *Ragone Relations for Thermal Energy Storage Technologies.* Front Mech Eng. 2019 Jun 4;5:29.

[12] Woods J, Mahvi A, Goyal A, Kozubal E, Odukomaiya A, Jackson R. *Rate capability and Ragone plots for phase change thermal energy storage.* Nat Energy. 2021 Mar;6(3):295–302.

https://doi.org/10.52202/069564-0193

[13] Shanks M, Shoalmire CM, Deckard M, Gohil KN, Lewis H, Lin D, et al. *Design of spatial variability in thermal energy storage modules for enhanced power density.* Applied Energy. 2022 May;314:118966.

[14] Curzon FL, Ahlborn B. *Efficiency of a Carnot engine at maximum power output.* American Journal of Physics. 1975 Jan;43(1):22–4.

[15] Coutier JP, Farber EA. *Two applications of a numerical approach of heat transfer process within rock beds.* Solar Energy. 1982;29(6):451–62.

[16] Anderson R, Bates L, Johnson E, Morris JF. *Packed bed thermal energy storage: A simplified experimentally validated model.* Journal of Energy Storage. 2015 Dec;4:14–23.

[17] Opitz F. *Packed bed thermal energy storage model - Generalized approach and experimental validation.* Applied Thermal Engineering. 2014;8.

[18] VDI e. V. *VDI Heat Atlas.* Berlin, Heidelberg: Springer Berlin Heidelberg; 2010.

[19] Incropera FP. *Fundamentals of heat and mass transfer.* 6th ed. Hoboken, NJ: John Wiley; 2007. 997 p.

[20] Ismail KAR, Jr RS. *A parametric study on possible packed bed models for PCM and sensible heat storage.* Applied Thermal Engineering. 1999;32.

[21] Meier A, Winkler C, Wuil D. *Experiment for modeling high temperature rock bed storage.* Solar Energy Materials. 1991;24(255–264):10.

[22] Allen KG, von Backström TW, Kröger DG. *Rock bed pressure drop and heat transfer: Simple design correlations.* Solar Energy. 2015 May;115:525–36.

[23] W. Neise, U. Michel. *Aerodynamic noise of turbomachines.* German Aerospace Center (DLR) Institute of Propulsion Technology, Department of Engine Acoustics; 1994. Report No.: Report 22314-94/B5.

[24] Schönholtz F, Grundmann, Reinhard, Eidam, Herbert, Rahn, Bernd. *Elementary Fan Technology.* TLT Turbo-GmbH; 2013.

[25] Menny K. *Strömungsmaschinen: hydraulische und thermische Kraft- und Arbeitsmaschinen.* 5th edition, Wiesbaden: Teubner; 2011. 327 p.

[26] Bard AJ, Faulkner LR. *Electrochemical methods: fundamentals and applications.* 2nd ed. New York: Wiley; 2001. 833 p.